Preprint: Supplementary Material for

Intrathecal antibodies cross-react with EBV BRRF2 and human antigens in multiple sclerosis

Poul M. Schulte-Frankenfeld,[1,2] Tim Decker,[1] Isabel Bünger,[1,2,3] Sarah Bamberg,[1,2] Manjusha Thakar,[4] William R. Morgenlander,[4] Patrick Schindler,[5] Carolin Otto,[5] Pia S. Sperber,[5,6] Tanja Schmitz-Hübsch,[7,8] Hans-Christian Kornau,[6,9] Dietmar Schmitz,[6,9] Sven Jarius,[10] Erin E. Longbrake,[11] Soumya Yandamuri,[11,12] Kevin C. O'Connor,[11,12] Carolin Schwake,[13] Ilya Ayzenberg,[13] Carlos A. Pardo,[4,14] Friedemann Paul,[5] Peter A. Calabresi,[14] Klemens Ruprecht,[10] H. Benjamin Larman[4,†] and Jakob Kreye[1,2,5,6,†]

[†]These authors contributed equally to this work.

Corresponding authors:

Jakob Kreye, MD

Department of Pediatric Neurology, Charité – Universitätsmedizin Berlin, corporate member of Freie Universität Berlin, Humboldt-Universität zu Berlin, and Berlin Institute of Health, Augustenburger Platz 1, 13353 Berlin, Germany.

E-mail: jakob.kreye@charite.de

and H. Benjamin Larman, Ph.D.

Johns Hopkins School of Medicine, Miller Research Building, Room 607, 733 North Broadway, Baltimore, MD 21205-1832

E-mail: hlarman1@jhmi.edu

Author affiliations:

1 Charité – Universitätsmedizin Berlin, corporate member of Freie Universität Berlin and Humboldt Universität zu Berlin, Department of Pediatric Neurology, Berlin, Germany

2 Berlin Institute of Health at Charité – Universitätsmedizin Berlin, Germany

3 Department of Surgery – Minimally Invasive and Visceral Surgery, Vivantes Klinikum Neukölln, Berlin, Germany

4 Institute for Cell Engineering, Division of Immunology, Department of Pathology, Johns Hopkins University School of Medicine, Baltimore, MD, USA

5 Charité – Universitätsmedizin Berlin, corporate member of Freie Universität Berlin and Humboldt-Universität zu Berlin, Department of Neurology and Experimental Neurology, Berlin, Germany

6 German Center for Neurodegenerative Diseases (DZNE) Berlin, Berlin, Germany

7 Experimental and Clinical Research Center, a cooperation between Max Delbrück Center (MDC) for Molecular Medicine in the Helmholtz Association, Charité – Universitätsmedizin Berlin, Berlin, Germany

8 Charité – Universitätsmedizin Berlin, corporate member of Freie Universität Berlin and Humboldt-Universität zu Berlin, Institute of Medical Immunology (IMI), Berlin, Germany

9 Charité – Universitätsmedizin Berlin, corporate member of Freie Universität Berlin and Humboldt-Universität zu Berlin, Neuroscience Research Center (NWFZ), Berlin, Germany

10 Division of Neuroimmunology, Department of Neurology, University of Heidelberg, Heidelberg, Germany

11 Department of Neurology, Yale University School of Medicine, New Haven, CT, USA

12 Department of Immunobiology, Yale University School of Medicine, New Haven, CT, USA

13 Ruhr University Bochum, Department of Neurology, St. Josef Hospital, Bochum, Germany

14 Department of Neurology, Johns Hopkins University School of Medicine, Baltimore, MD, USA

SUPPLEMENTARY FIGURES

Supplementary Figure 1: Viral antibody responses in serum, CSF and intrathecal synthesis

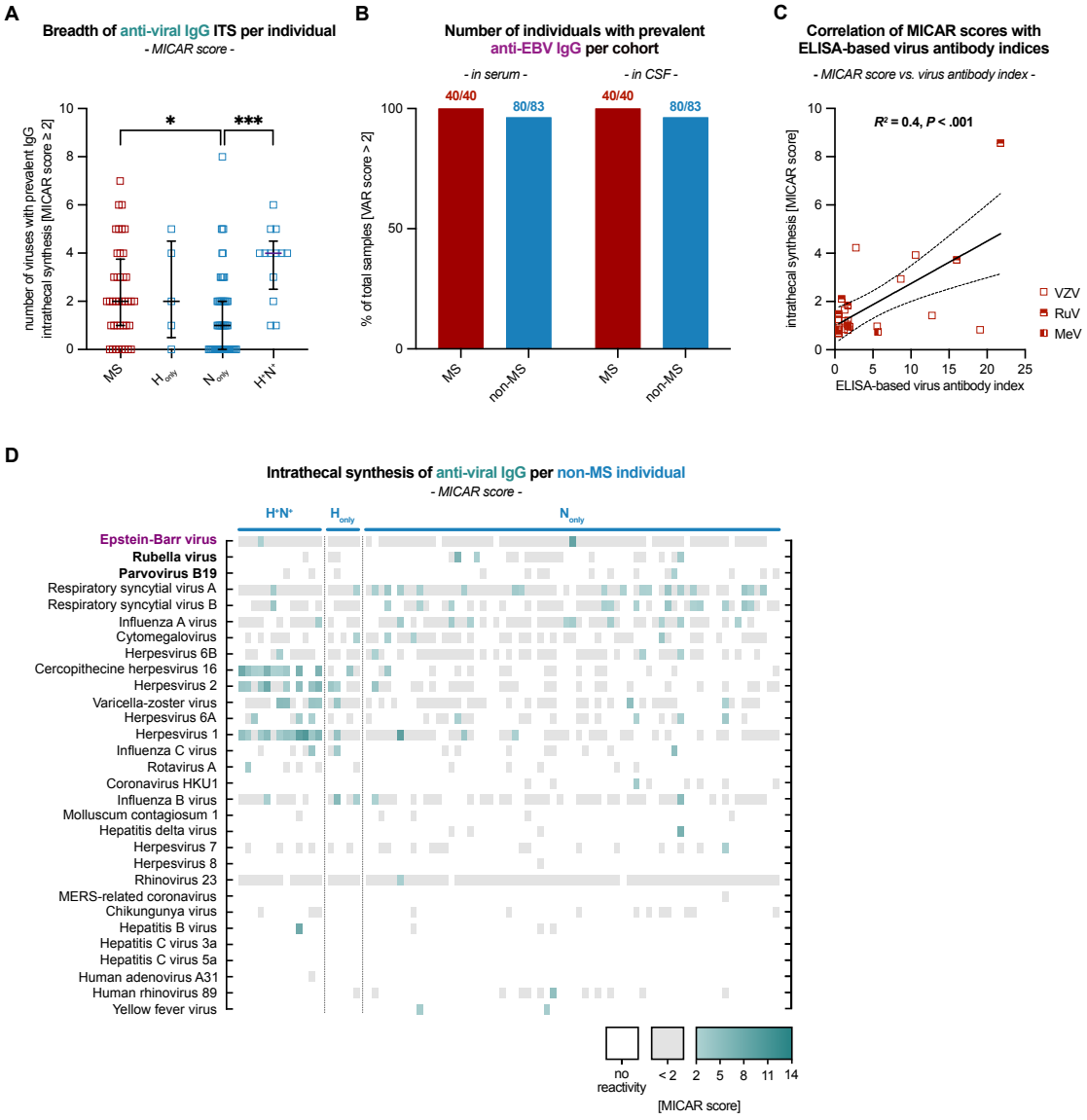

(A) Number of viruses with detectable intrathecal antibody enrichment in each individual (MICAR score > 2). Each square represents one individual in the MS cohort (*n* = 40) and non-MS subgroups (H_{only}: *n* = 5, N_{only}: *n* = 65, H^+N^+: *n* = 13). Group differences were assessed using a Kruskal–Wallis test (*P* < .0001) with Dunn's post-hoc, only significant post-hoc tests are indicated by asterisks; horizontal lines indicate the median, whiskers indicate the interquartile range.

(**B**) Number of individuals with a detectable response against Epstein-Barr Virus (EBV) peptides (VAR score > 2) per cohort in serum and CSF.

(**C**) Individual-level intrathecal antibody enrichment quantification measured using MICAR scores, correlated with corresponding intrathecal antibody enrichment measures from routine clinical ELISA-

based antibody indices for MRZ viruses: measles virus (MeV), rubella virus (RuV) and varicella-zoster virus (VZV), in individuals with MS (MeV: $n = 3$, RuV: $n = 7$, VZV: $n = 15$). Each square represents one individual's measurement for a given virus, some individuals had data available for multiple viruses. The x-axis shows the ELISA-based clinical antibody index; the y-axis shows the MICAR score. MICAR scores and ELISA-based antibody indices are positively associated in a linear regression model ($R^2 = 0.4$, $P < .001$). Dashed lines indicate 95% confidence intervals.

(**D**) Extension of Fig. 1G. Individual-level heatmap of intrathecal virus-specific antibody synthesis in non-MS individuals (total: $n = 83$; thereof H^+N^+: $n = 13$, H_{only}: $n = 5$, N_{only}: $n = 65$), quantified by MICAR scores. Only viruses with ITS in at least one MS individual are shown. White indicates absence of detectable CSF reactivity; grey indicates detectable but not intrathecally enriched reactivity; and green indicates intrathecally enriched reactivity, with darker shades corresponding to higher ITS magnitude.

Supplementary Figure 2: Peptide-level intrathecal antibody synthesis

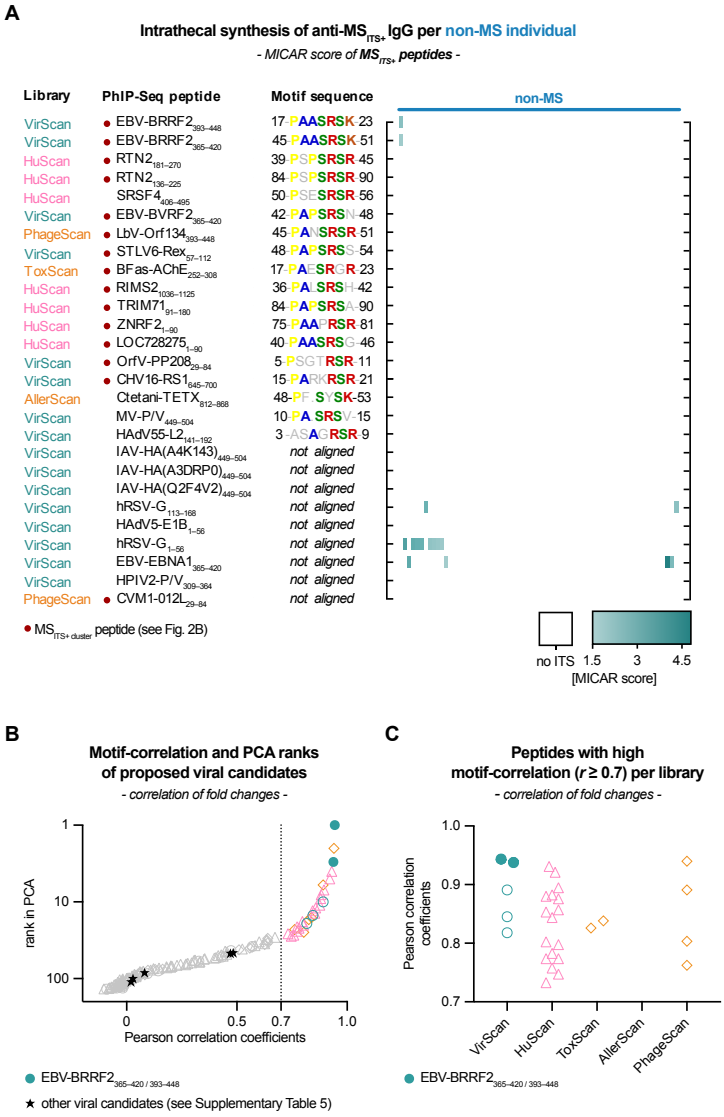

(**A**) Extension of Fig. 2D. Individual-level heatmap of MICAR scores for MS_{ITS+} peptides in individuals with MS (*n* = 40), grouped by MS_{IC} status. White indicates absence of ITS; shades of green indicate magnitude of ITS. Motif sequences represent aligned central peptide regions. Colored residues indicate agreement with the IC-motif; grey residues indicate no agreement.

(**B**) Modified version of Fig. 2E. Correlation analysis of antibody binding among PhIP-Seq library peptides containing a motif with up to one amino acid mismatch to the IC-motif (n = 300 peptides) and binding in at least one sample (n = 137/300 peptides). Each symbol represents one peptide; colors and shapes are as in Fig. 2A. The x-axis shows Pearson correlation coefficients for the five highest-ranking peptides across all samples; the y-axis indicates rank based on the first principal component. Peptides with correlations $r \geq 0.7$ (*n* = 28) were reanalyzed for sequence alignment. Peptides proposed as potential viral candidates for the IC-motif by previous reports (see Supplementary Table 5) are labeled with a star.

(**C**) PhIP-Seq library origin of motif-correlated peptides ($r \geq 0.7$; $n = 28$), showing that the correlation cluster is predominantly composed of human protein-derived peptides, with EBV BRRF2 as the major viral contributor. Each symbol represents one peptide; colours and shapes are as in Fig. 2A. The x-axis indicates the PhIP-Seq library from which each peptide was derived, and the y-axis shows Pearson correlation coefficients relative to the five highest-ranking peptides across all samples.

Supplementary Figure 3: Characterization of CSF reactivity across proteomes of motif-correlated $MS_{ITS+\ cluster}$ peptides

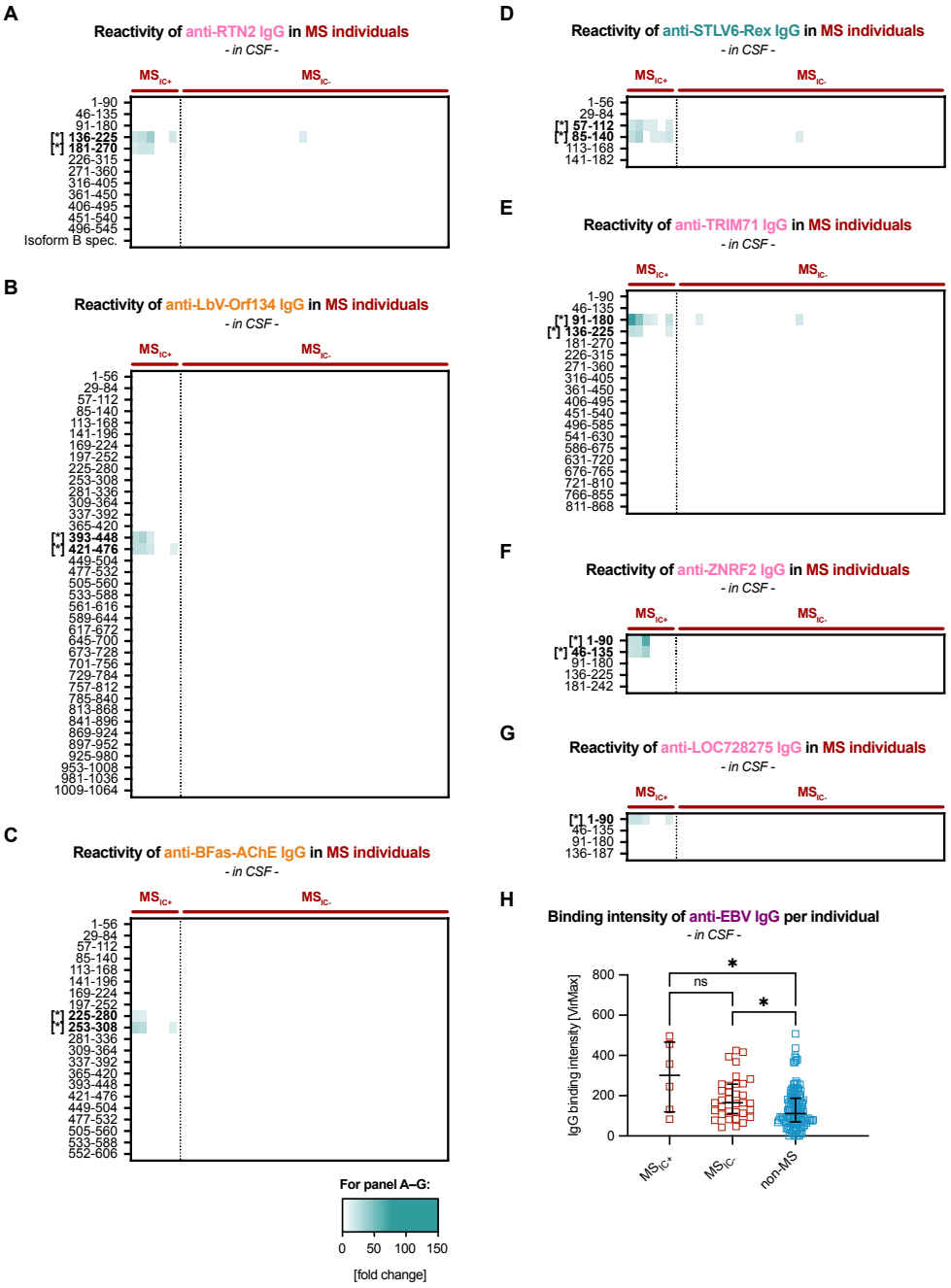

(**A–G**) Individual-level heatmaps of CSF reactivity across proteomes of proteins associated with $MS_{ITS+\ cluster}$ peptides with motif-correlation ($r \geq 0.7$) in addition to Fig. 3C showing CSF reactivity for the EBV BRRF2 protein. Each panel displays one protein, including human proteins RTN2 (A), TRIM71 (E), ZNRF2 (F) and LOC728275 (G) (see Supplementary Table 4 for protein names and associated pathogens). Rows correspond to separate tiles as represented in the PhIP-Seq library. Positions within proteins indicated with an asterisks indicating IC-motif containing peptides. Columns represent

individuals stratified by MS_{IC} status (MS_{IC+}: n = 6, MS_{IC-}: n = 34). White indicates absence of detectable reactivity; shades of green indicate magnitude of antibody binding intensity.

(**H**) Individual-level EBV-specific CSF antibody binding intensity, measured as VirMax, stratified by MS_{IC} status. Each square represents one individual (MS_{IC+}: n = 6, MS_{IC-}: n = 34, non-MS: n = 83). Group differences were assessed using a Kruskal–Wallis test (P < .01) with Dunn's post-hoc. Horizontal lines indicate the median; whiskers indicate the interquartile range. Illustration is related to Fig. 1F.

Supplementary Figure 4: Validation of an ELISA-based serum IgG motif testing protocol

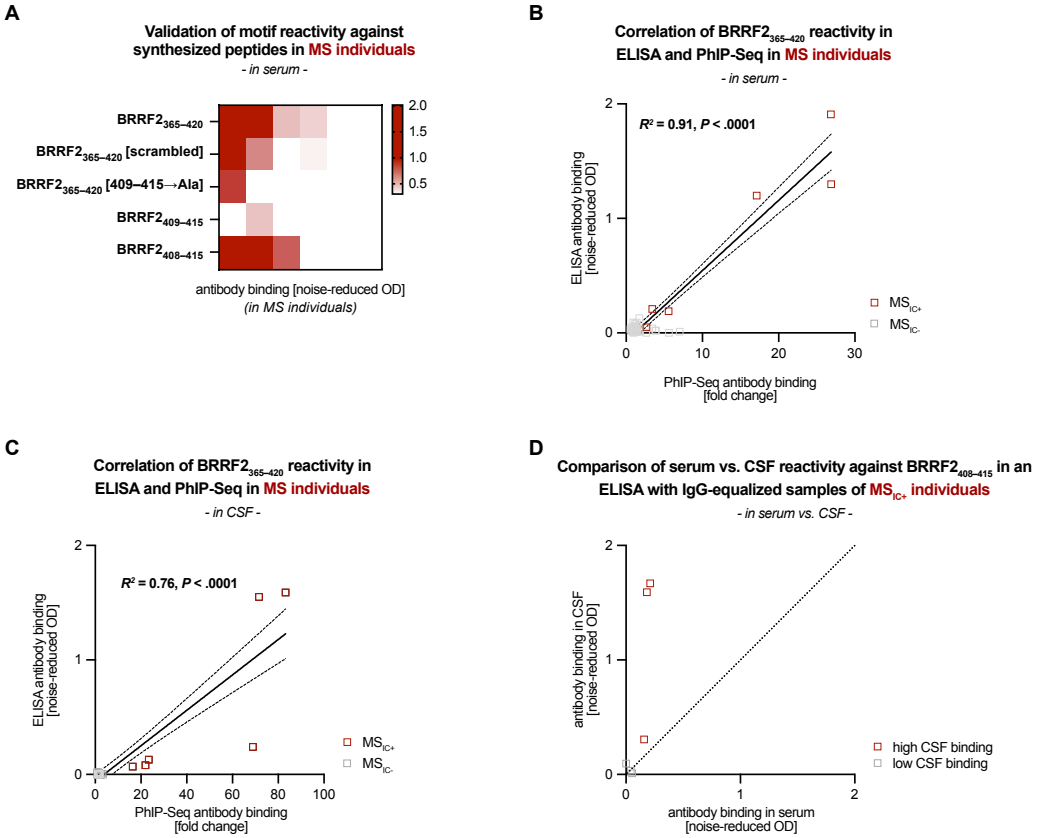

(A) Individual-level heatmap of ELISA-based serum IgG reactivity against peptides derived from the 56-mer PhIP-Seq sequence (BRRF2$_{365–420}$), including: the full-length peptide; a variant in which the central PAASRSK motif scrambled to SSPKARA (BRRF2$_{365–420}$[scrambled]); an alanine-substituted variant in which residues 409–415 were replaced by alanines (BRRF2$_{365–420}$[409–415→Ala]; the isolated core motif (BRRF2$_{409–415}$); and an extended variant including one additional N-terminal residue (BRRF2$_{408–415}$). See Supplementary Table 3 for a full list of peptides. Columns represent individuals with MS (n = 6). Shades of Red indicate magnitude of noise-reduced OD.

(**B**) Individual-level ELISA-based serum IgG reactivity against BRRF2$_{365–420}$ correlated with PhIP-Seq binding intensity against the BRRF2$_{365–420}$ tile. Each square represents one individual stratified by MS$_{IC}$ status (MS$_{IC+}$: n = 6, MS$_{IC-}$: n = 34) The x-axis shows PhIP-Seq binding intensity (fold change); the y-axis shows ELISA reactivity (noise-reduced OD). ELISA-based and PhIP-Seq-based serum reactivity to BRRF2$_{365–420}$ are positively associated in a linear regression model (R^2 = 0.91, P < .0001). Dashed lines indicate 95% confidence intervals.

(**C**) Corresponding analysis to (B) in CSF. ELISA-based and PhIP-Seq-based CSF reactivity to BRRF2$_{365–420}$ are positively associated in a linear regression model (R^2 = 0.76, P < .0001). Dashed lines indicate 95% confidence intervals.

(**D**) Individual-level ELISA-based IgG reactivity to $BRRF2_{408–415}$ in paired, IgG-normalized serum and CSF samples from MS_{IC+} individuals (*n* = 6). Total IgG levels were quantified using a commercial IgG ELISA, and serum samples were diluted to match the corresponding CSF IgG concentration. IgG-matched samples were then assessed for $BRRF2_{408–415}$ reactivity. The x-axis shows noise-reduced OD in serum and the y-axis in CSF. Each square represents one individual; samples with high PhIP-Seq binding intensity to $BRRF2_{365–420}$ in CSF are shown in red (fold change ≥ 25), and those with lower binding intensity in grey (fold change < 25). The dotted line indicates the line of identity (45°); values above the line indicate relatively higher IgG levels of $BRRF2_{408–415}$-specific IgG in CSF compared to serum.

Supplementary Figure 5: Exploration of EBV-motif co-reactivities, temporal stability and clinical associations

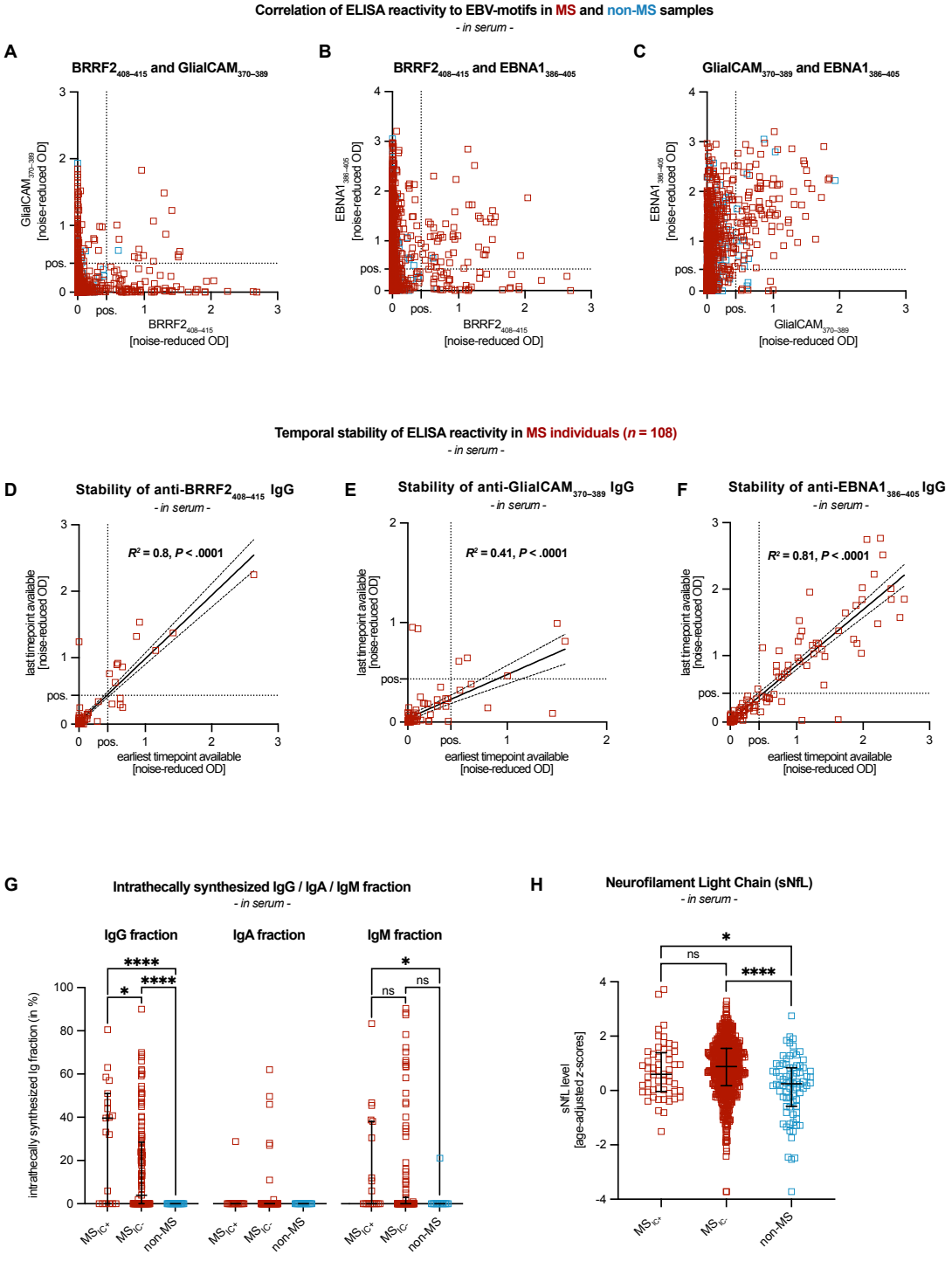

(**A–C**) Individual-level ELISA-based serum IgG reactivity to BRRF2$_{408–415}$, GlialCAM$_{370–389}$, and EBNA1$_{386–405}$. Each square represents one individual (MS: *n* = 909, non-MS: *n* = 311). The x- and y-axes show noise-reduced OD for the indicated peptide pairs.

(**D–F**) Temporal stability of ELISA-based serum IgG reactivity to $BRRF2_{408–415}$, $GlialCAM_{370–389}$, and $EBNA1_{386–405}$ peptides, respectively. Each square represents one MS individual with available longitudinal samples (n = 108). The x-axis shows the noise-reduced OD at the earliest available timepoint, and the y-axis shows noise-reduced OD at the last available timepoint. ELISA-based IgG reactivity measurements at both timepoints are positively correlated in a linear regression model for $BRRF2_{408–415}$ (R^2 = 0.8, P < .0001), $GlialCAM_{370–389}$ (R^2 = 0.41, P < .0001) and $EBNA1_{386–405}$ (R^2 = 0.81, P < .0001).

(**G**) Individual-level intrathecal synthesis fractions of IgG, IgA and IgM measurements stratified by MS_{IC} status. Each square represents one individual with varying data availability for IgG (MS_{IC+}: n = 19, MS_{IC-}: n = 121, non-MS: n = 26), for IgA (MS_{IC+}: n = 19, MS_{IC-}: n = 116, non-MS: n = 19) and for IgM (MS_{IC+}: n = 19, MS_{IC-}: n = 116, non-MS: n = 15). Group differences were assessed using a Kruskal–Wallis test (IgG: P < .0001; IgA: P = .55, IgM: P < .05) with Dunn's post-hoc where appropriate. Horizontal lines indicate the median; whiskers indicate the interquartile ranges.

(**H**) Individual-level age-adjusted z-scores for serum Neurofilament Light Chain (sNfL) measurements stratified by MS_{IC} status. Each square represents one individual (MS_{IC+}: n = 54, MS_{IC-}: n = 646, non-MS (all HC/OND): n = 78). Group differences were assessed using a Kruskal–Wallis test (P < .0001) with Dunn's post-hoc. Horizontal lines indicate the median; whiskers indicate the interquartile ranges.

SUPPLEMENTARY TABLES

Supplementary Table 1: Sample characteristics of the discovery cohort

			non-MS per subgroup[a]		
Variables	**MS**	**non-MS**	**H^+N^+**	**H_{only}**	**N_{only}**
Number of individuals, n	40	83	13	5	65
Sample characteristics					
Age in years, median (IQR)	33.5 (28–39)	32 (22–42)	64 (38–75)	32 (24.5–50.5)	29 (21–35.5)
Sex, %Female	67.5%	74.7%	61.5%	80%	76.9%
Months since symptom onset, median (IQR)	6 (1–23)	4 (0–24)	2 (0–6.5)	36 (0–184)	7 (0–24)
Geographic distribution					
Germany, n (% of total)	40 (100%)	81 (97.6%)	13 (100%)	3 (60%)	65 (100%)
CSF parameters					
CSF WBC in cells/µL, median (IQR)	10 (5–18)	3 (1–12)	5 (2–32.5)	8 (3–39)	3 (1–8)
CSF Protein in mg/L, median (IQR)	352 (270–421)	n/a	n/a	n/a	n/a
Age-adjusted Qalb, median (IQR)	0.7 (0.5–0.9)	0.7 (0.5–1)	0.8 (0.6–1.6)	0.4 (0.2–4.2)	0.7 (0.5–1)
CSF-specific Oligoclonal Bands, %	100%	48.2%	69.2%	40%	44.6%
Intrathecal Synthesis parameters					
Intrathecal IgG synthesis in %, median (IQR)	25 (8.5–46.5)	0 (0–19.1)	40.4 (0–45.8)	0 (0–19.2)	0 (0–0)
Intrathecal IgG synthesis >10%, %	72.5%	26.5%	69.2%	20%	18.5%

[a] As non-MS controls, we used samples from patients with NMDARE or HSE, abbreviated as follows: HSE only (H_{only}), NMDARE only (N_{only}), HSE and secondary NMDARE (H^+N^+)

Supplementary Table 2: Sample characteristics of the validation cohort

			non-MS per subgroup			
Variables	**MS**	**non-MS**	**NMOSD**	**MOGAD**	**HC/OND**	**Data availability per variable[a]**
Number of individuals, n	909	311	78	93	140	
follow-up measurement available, n	108	0	0	0	0	
Sample characteristics						
Age in years, median (IQR)	48 (37–57)	48 (36–59)	55 (43–63)	35 (27–48)	53 (42–60)	[848, 218 (50, 71, 97)]
Sex, %Female	72.9%	64.1%	92.2%	61.1%	51.5%	[848, 220 (51, 72, 97)]
Months since diagnosis, median (IQR)	108 (48–192)	n/a	42 (15–111)	23 (5–64)	n/a	[847, n/a (50, 70, n/a)]
Geographic distribution						
Germany, n (% of total)	149 (16%)	184 (51%)	51 (65%)	73 (78%)	60 (31%)	[909, 311 (78, 93, 140)]
Clinical characteristics						
EDSS, median (IQR)	3 (1.5–3.5)	2.75 (1.5–4)	3.5 (2–4.5)	2 (1.5–3.5)	n/a	[734, 69 (33, 36, n/a)]
Serum NfL in pg/mL, median (IQR)	11.1 (8.7–15)	10.8 (7.3–13.9)	n/a	n/a	10.8 (7.3–13.9)	[700, 79 (n/a, n/a, 79)]
Serum NfL age-adjusted z-score, median (IQR)	0.9 (0.2–1.5)	0.3 (-0.5–0.9)	n/a	n/a	0.3 (-0.5–0.9)	[700, 79 (n/a, n/a, 79)]
CSF parameters						
CSF WBC in cells/µL, median (IQR)	5 (3–11)	7.5 (2.3–13.8)	3 (1.5–15.5)	8 (2.5–22)	n/a	[102, 30 (9, 21, n/a)]
CSF Protein in mg/L, median (IQR)	n/a	365 (334–442)	399 (242–437)	358 (337–444)	n/a	[n/a, 22 (5, 17, n/a)]
Age-adjusted Qalb, median (IQR)	0.8 (0.6–1)	0.8 (0.7–1)	0.8 (0.7–1.2)	0.8 (0.7–1)	n/a	[99, 17 (3, 14, n/a)]
CSF-specific Oligoclonal Bands, %	89.2%	16.7%	17.6%	13%	n/a	[102, 63 (17, 46, n/a)]
Intrathecal Synthesis parameters						

Intrathecal IgG synthesis in %, median (IQR)	0 (0–26.4)	0 (0–0)	0 (0–0)	0 (0–0)	n/a	[100, 26 (7, 19, n/a]
Intrathecal IgA synthesis in %, median (IQR)	0 (0–0)	0 (0–0)	0 (0–0)	0 (0–0)	n/a	[95, 19 (3, 16, n/a)]
Intrathecal IgM synthesis in %, median (IQR)	0 (0–0.8)	0 (0–0)	0 (0–0)	0 (0–0)	n/a	[98, 15 (3, 12, n/a)]

[a] Number of samples with available data for each respective variable. Format: [MS, non-MS (NMOSD, MOGAD, HC/OND)]

Abbreviations: CSF = cerebrospinal fluid; EDSS = Expanded Disability Status Scale; IgA/G/M = immunoglobulin A/G/M; IQR = interquartile range; MS = multiple sclerosis; MS_{IC} = MS immunogenic cluster; NfL = neurofilament light chain; OCB = oligoclonal band; QAlb = albumin quotient; WBC = white blood cell count.

Supplementary Table 3: List of synthesized peptides

Name	Modifications	Length	Sequence
BRRF2 constructs			
BRRF2$_{365–420}$	His-Tag, Strep-Tag II	56 + 16	PPVCPIVSLTASGAKQNRGGMGSLHLAKPEETSPAVSPVCP IASPAASRSKQHCGVHHHHHHSAWSHPQFEK-COOH
BRRF2$_{365–420}$ scrambled	His-Tag, Strep-Tag II	56 + 16	PPVCPIVSLTASGAKQNRGGMGSLHLAKPEETSPAVSPVCP IASSSPKARAQHCGVHHHHHHSAWSHPQFEK-COOH
BRRF2$_{365–420}$ alanine-substituted	His-Tag, Strep-Tag II	56 + 16	PPVCPIVSLTASGAKQNRGGMGSLHLAKPEETSPAVSPVCP IASAAAAAAAQHCGVHHHHHHSAWSHPQFEK-COOH
BRRF2$_{409–415}$	His-Tag, Strep-Tag II	7 + 16	PAASRSKHHHHHHSAWSHPQFEK-COOH
BRRF2$_{408–415}$	His-Tag, Strep-Tag II	8 + 16	SPAASRSKHHHHHHSAWSHPQFEK-COOH
EBNA1-mimic constructs			
GlialCAM$_{370–389}$	His-Tag, Strep-Tag II, pSer376	20 + 16	ATGRTHSpSPPRAPSSPGRSRHHHHHHSAWSHPQFEK-COOH
EBNA1$_{386–405}$	His-Tag, Strep-Tag II	20 + 16	SQSSSSGSPPRRPPPGRRPFHHHHHHSAWSHPQFEK-COOH
Human protein constructs			
TRIM71$_{173–180}$	His-Tag, Strep-Tag II	8 + 16	PPAPSRSAHHHHHHSAWSHPQFEK-COOH
RTN2$_{218–225}$	His-Tag, Strep-Tag II	8 + 16	TPSPSRSRHHHHHHSAWSHPQFEK-COOH
ZNRF2$_{74–81}$	His-Tag, Strep-Tag II	8 + 16	APAAPRSRHHHHHHSAWSHPQFEK-COOH
RIMS2$_{1080–1087}$	His-Tag, Strep-Tag II	8 + 16	SPALSRSHHHHHHSAWSHPQFEK-COOH
Technical constructs			
His-Strep-Tag II		16	HHHHHHSAWSHPQFEK-COOH

Supplementary Table 4: List of MS_{ITS+} peptides

					Network Analysis	
Peptide Name	**Library**	**Species**	**UniProt ID**	**Sequence**	**Node Centrality**	**Cluster**
EBV-BRRF2$_{393–448}$	VirScan	Epstein-Barr virus	Q1HVF8	PEETSPAVSPVCPIASPAASRSKQHCGVTGSSQAA PSSSSVAPVASLSGDLEEEEE	6.00	1
EBV-BRRF2$_{365–420}$	VirScan	Epstein-Barr virus	Q1HVF8	PPVCPIVSLTASGAKQNRGGMGSLHLAKPEETSPA VSPVCPIASPAASRSKQHCGV	4.05	1
RTN2$_{181–270}$	HuScan	Homo sapiens	O75298	TGEAGEELDLRLRLAQPSSPEVLTPQLSPGSGTPQ AGTPSPSRSRDSNSGPEEPLLEEEEKQWGPLEREP VRGQCLDSTDQLEFTVEPRL	5.82	1
RTN2$_{136–225}$	HuScan	Homo sapiens	O75298	PLEDLRLRLDHLGWVARGTGSGEDSSTSSSTPLED EEPQEPNRLETGEAGEELDLRLRLAQPSSPEVLTP QLSPGSGTPQAGTPSPSRSR	7.05	1
SRSF4$_{406–495}$	HuScan	Homo sapiens	Q08170	SPSRSVSKEREHAKSESSQREGRGESENAGTNQE TRSRSRSNSKSKPNLPSESRSRSKSASKTRSRSKS RSRSASRSPSRSRSRSHSRS	0.00	4
EBV-BVRF2$_{365–420}$	VirScan	Epstein-Barr virus	Q1HVC7	DAHTYHPHPHPPPAYFGLPGLFGPPPPVPPYYGSH LRADYVPAPSRSNKRKRDPEE	6.16	1
LbV-Orf134$_{393–448}$	PhageScan	Phage (Lactobacillus virus LP65)	YP_164769.1	KKVNPKGSWSKSRKTSENGEPDWTPYILAIIDTEHK LNSSSQSDPANSRSRGSASS	4.69	1
STLV6-Rex$_{57–112}$	VirScan	Simian T-cell lymphotropic virus	D1MNA2	PPGYIGTPYWPPVLNTRSPGTPSMDALSARLYNTLS LASPPSPPKELPAPSRSSPR	5.86	1
BFas-AChE$_{252–308}$	ToxScan	Bungarus fasciatus	Q92035	AILQSGGPNAPWATVTPAESRGRAALLGKQLGCHF NNDSELVSCLRSKNPQELIDE	4.87	1
RIMS2$_{1036–1125}$	HuScan	Homo sapiens	Q9UQ26	LLERTTTRSRSTERPDTNLMRSMPSLMTGRSAPPS PALSRSHPRTGSVQTSPSSTPVAGRRGRQLPQLPP KGTLDRKAGGKKLRSTVQRS	6.47	1
TRIM71$_{91–180}$	HuScan	Homo sapiens	Q2Q1W2	CPVCDQKVVLAEAAGMDALPSSAFLLSNLLDAVVAT ADEPPPKNGRAGAPAGAGGHSNHRHHAHHAHPRA SASAPPLPQAPQPPAPSRSA	7.67	1
ZNRF2$_{1–90}$	HuScan	Homo sapiens	Q8NHG8	MGAKQSGPAAANGRTRAYSGSDLPSSSSGGANGT AGGGGGARAAAAGRFPAQVPSAHQPSASGGAAAA AAAPAAPAAPRSRSLGGAVGSV	6.33	1
LOC728275$_{1–90}$	HuScan	Homo sapiens	n/a	MPAHHDPQILDGDSGEEAETTTPQCGTEPPSSGLKI SAIPAASRSGPGASPTVNTDPGLLPKWGREQAASR ETGWKGLSPTTASLPLLRG	8.56	1
OrfV-PP208$_{29–84}$	VirScan	Parapoxvirus / Orf virus	F1AX61	TSRTPSGTRSRAKYRAGTGSGARPCGPWASACGP CSCWSWRSLRAMTASRPWPALW	2.87	1

CHV16-RS1$_{645–700}$	VirScan	Cercopithecine herpesvirus 16	Q2QBA3	SSSPPRAPAPAARPPARKRSRPARPRPPGAPADDDDDNGGGRARAPGPRPRPAALT	6.75	1
Ctetani-TETX$_{812–868}$	ToxScan	Clostridium tetani	P04958	AKKQLLEFDTQSKNILMQYIKANSKFIGITELKKLESKINKVFSTPIPFSYSKNLD	0.00	9
MV-P/V$_{449–504}$	VirScan	Measles virus	P35974	AVGFVPDTGPASRSVIRSIIKSSRLEEDRKRYLMTLLDDIKGANDLAKFHQMLMKI	0.00	8
HAdV55-L2$_{141–192}$	VirScan	Human adenovirus type 55	C7SRT6	SGASAGRSRRQAAAVAAATIADMAQTRRGNVYWVRDAATGQRVPVRTRPPRT	0.00	5
IAV-HA(A4K143)$_{449–504}$	VirScan	Influenza A virus	A4K143	ERTLDFHDSNVKNLYEKVKNQLRNNAKEIGNGCFEFYHKCDNECMESVKNGTYDYP	1.93	2
IAV-HA(A3DRP0)$_{449–504}$	VirScan	Influenza A virus	A3DRP0	ERTLDFHDSNVKNLYEKVKNQLKNNAKEIGNGCFEFYHKCNNECMESVKNGTYDYP	1.91	2
IAV-HA(Q2F4V2$_{449–504}$	VirScan	Influenza A virus	Q2F4V2	NERTLDFHDSNVKNLYDKVRLQLRDNAKELGNGCFEFYHKCDNECMESVRNGTYDY	1.90	2
hRSV-G$_{113–168}$	VirScan	Human respiratory syncytial virus	E9NW54	PCSICSNNPTCWAICKRIPNKKPGKKTTTKPTKKPTIKTTKKDPKPQTTKPKEVLT	0.00	10
HAdV5-E1B$_{1–56}$	VirScan	Human adenovirus C serotype 5	P03243	MERRNPSERGVPAGFSGHASVESGCETQESPATVVFRPPGDNTDGGAAAAAGGSQA	0.00	6
hRSV-G$_{1–56}$	VirScan	Human respiratory syncytial virus	C1K8X5	PAQTNRPSTKPRPKNPPKKPKDDYHFEVFNFVPCSICGNNQLCKSICKTIPSNKPK	0.00	7
EBV-EBNA1$_{365–420}$	VirScan	Epstein-Barr virus	Q1HVF7	SRERARGRGRGRGEKRPRSPSSQSSSSGSPPRRPPPGRRPFFHPVAEADYFEYHQE	0.53	3
HPIV2-P/V$_{309–364}$	VirScan	Human parainfluenza type 2 virus	P23055	SGGFTAEGSDMISMDELARPTLSSTKRITRKPESKKDLTGIKLTLMQLANDCISRP	0.53	3
CVM1-012L$_{29–84}$	PhageScan	Phage (Paramecium bursaria Chlorella virus)	AGE51696	TTSDVKMPSKFTVDKWKYNKSVLPFYDTRDYEESRQGLMATPAYKQIKDADGKVVW	7.16	1

Supplementary Table 5: Motif score correlation

					IC-motif correlation analysis	
Peptide Name	**Library**	**Associated Species**	**UniProt ID**	**IC-motif Pattern**	**Correlation Coefficient**	**FPC Rank[a]**
Peptides with IC-motif correlation scores ≥ 0.7						
EBV-BRRF2$_{393–448}$	VirScan	Epstein-Barr virus	Q1HVF8	PAASRSK	0.943608	1
LbV-Orf134$_{421–477}$	HuScan	Homo sapiens	YP_164769.1	PANSRSR	0.9398	2
EBV-BRRF2$_{365–420}$	VirScan	Epstein-Barr virus	Q1HVF8	PAASRSK	0.937504	3
KRT75$_{1–91}$	HuScan	Homo sapiens	O95678	PAAGRSR	0.930814	4
LOC728275$_{1–91}$	HuScan	Homo sapiens	n/a	PAASRSG	0.921057	5
CFAP97$_{46–136}$	HuScan	Homo sapiens	Q9P2B7	PASSRSK	0.894666	7
LbV-Orf134$_{393–449}$	PhageScan	Phage (Lactobacillus virus LP65)	YP_164769.1	PANSRSR	0.890959	6
STLV6-Rex$_{57–112}$	VirScan	Simian T-cell lymphotropic virus	D1MNA2	PAPSRSS	0.89081	10
RTN2$_{181–271}$	HuScan	Homo sapiens	O75298	PSPSRSR	0.882711	8
LOC100287739$_{1–91}$	HuScan	Homo sapiens	n/a	PSRSRSR	0.880118	9
K2C75$_{1–56}$	HuScan	Homo sapiens	O95678	PAAGRSR	0.87583	11
TRIM71$_{136–226}$	HuScan	Homo sapiens	Q2Q1W2	PAPSRSA	0.857275	12
TRIM71$_{91–181}$	HuScan	Homo sapiens	Q2Q1W2	PAPSRSA	0.85335	14
STLV6-Rex$_{85–140}$	VirScan	Simian T-cell lymphotropic virus	D1MNA2	PAPSRSS	0.845473	15
CFAP97$_{91–181}$	HuScan	Homo sapiens	Q9P2B7	PASSRSK	0.844051	13
BFas-AChE$_{252–308}$	ToxScan	Bungarus fasciatus	Q92035	PAESRGR	0.838344	16
CAlb-WOR2_CANAL$_{56–112}$	ToxScan	Candida albicans	Q5ANB1	PSPGRSK	0.82613	17

HHV1$_{29–81}$	VirScan	Human herpesvirus 1	Q6VB60	PAASRSV	0.817885	19
StrmV-VWB$_{57–113}$	PhageScan	Phage (Streptomyces phage VWB)	NP_958294.1	PATSRSK	0.803416	25
RTN2$_{136–226}$	HuScan	Homo sapiens	O75298	PSPSRSR	0.802219	20
ZNRF2$_{46–136}$	HuScan	Homo sapiens	Q8NHG8	PAAPRSR	0.797741	18
FOXO6$_{406–496}$	HuScan	Homo sapiens	n/a	PAPSRSA	0.782512	22
DENND4C$_{1036–1126}$	HuScan	Homo sapiens	Q5VZ89	PAVSRSK	0.773939	24
FOXO6$_{319–388}$	HuScan	Homo sapiens	n/a	PAPSRSA	0.773893	21
EMas$_{29–85}$	PhageScan	Eisenbergiella massiliensis	WP_117531915.1	PAPPRSK	0.762369	23
TYSND1$_{46–136}$	HuScan	Homo sapiens	Q2T9J0	PAPSRGR	0.757875	27
FOXO6$_{451–541}$	HuScan	Homo sapiens	n/a	PAPSRSA	0.747287	28
CLASRP$_{496–586}$	HuScan	Homo sapiens	Q8N2M8	LSPSRSR, PSQSRSR, PSPSQSR, PSRSRSL	0.732510	26
Other viral candidates hypothesized in prior work[b]						
EBV-gM$_{309–364}$	VirScan	Epstein-Barr virus	P03215	PSPGRNR	0.483267	46
EBV-gM$_{337–392}$	VirScan	Epstein-Barr virus	P03215	PSPGRNR	0.470714	47
REBOV-VP30$_{1–56}$	VirScan	Reston ebolavirus (Phillipines-96)	Q91DD6	PSRSRSL	0.081692	84
HCV6h$_{1093–1148}$	VirScan	Hepatitis C virus genotype 6h	O92532	PAGARSL	0.028485	100
REBOV-VP30$_{1–56}$	VirScan	Reston ebolavirus (Reston-89)	Q8JPX6	PSRSRSL	0.019791	110

[a] Rank in the first principal component of a PCA on relative binding scores of 137/300 peptides which bound in at least one sample across all CSF and serum samples from MS and non-MS cohorts. See *Materials and methods* and Fig. 2A.
[b] see Zamecnik CR, Sowa GM, Abdelhak A, et al. An autoantibody signature predictive for multiple sclerosis. *Nat Med*. 2024;30(5):1300-1308. doi:10.1038/s41591-024-02938-3

Supplementary Table 6: Association of ELISA-based anti-motif IgG seropositivity with MS diagnosis

Predictor	Odds ratio	95% Confidence Interval	*P*-value	Samples included[a]	Number of events[a]
Unadjusted logistic regression					
$BRRF2_{408–415}$	14.1	4.4–86.04	.0002	1220	909
$GlialCAM_{370–389}$	2.81	1.58–5.46	.001	1220	909
$EBNA1_{386–405}$	2.23	1.69–2.95	< .0001	1220	909
Unadjusted Firth penalized logistic regression					
$BRRF2_{408–415}$	11.4	3.91–54.9	< .0001	1220	909
$GlialCAM_{370–389}$	2.71	1.54–5.21	.0003	1220	909
$EBNA1_{386–405}$	2.22	1.68–2.94	< .0001	1220	909
Adjusted Firth penalized logistic regression[b]					
$BRRF2_{408–415}$	9.48	3.12–46.8	< .0001	1064	846
$GlialCAM_{370–389}$	3.61	1.7–8.63	.0005	1064	846
$EBNA1_{386–405}$	2.54	1.76–3.72	< .0001	1064	846

[a] Adjusted analyses were restricted to complete cases across all included variables, thus number of included samples and events (samples from individuals with MS diagnosis) are reduced in comparison to Fig. 4A.

[b] Adjusted for age, sex and country of sampling.

Supplementary Table 7: Associations between ELISA-based anti-motif IgG seropositivity measures

Predictor	Odds ratio	95% Confidence Interval	*P*-value	Samples included[a]	Number of events[a]
Adjusted Firth penalized logistic regression on EBNA1$_{386–405}$[b]					
BRRF2$_{408–415}$	1.45	0.87–2.44	.1568	1064	442
GlialCAM$_{370–389}$	19.72	9.86–45.94	< .0001	1064	442
Adjusted Firth penalized logistic regression on BRRF2$_{408–415}$[b]					
GlialCAM$_{370–389}$	1.81	0.9–3.46	.0929	1064	74
EBNA1$_{386–405}$	1.45	0.86–2.43	.162	1064	74

[a] Adjusted analyses were restricted to complete cases across all included variables, thus number of included samples and events (seropositive samples) are reduced in comparison to Fig. 4A.

[b] Adjusted for age, sex, country of sampling and disease group (MS / non-MS)

Supplementary Table 8: Human Protein List[a]

Gene name	Gene Product	UniProt ID	Predicted Location	Tissue profile	Tissue specificity	Single cell type specificity	Brain specificity	Brain expression cluster	Phenotype from variants (MIM #)
RTN2	Reticulon-2 / Neuroendocrine-specific protein-like	O75298	Membrane	Cytoplasmic expression in muscle cells	Skeletal muscle, tongue	Extravillous trophoblasts, Cytotrophoblasts, Platelets, Syncytiotrophoblasts, Migrating cytotrophoblasts, Myonuclei	Low	Neurons & Synapses - Synaptic function (mainly)	Spastic paraplegia 12 (604805)
KRT75 (K2C75)	Keratin, type II cytoskeletal 75	O95678	Intracellular	Distinct cytoplasmic expression in the outer root sheath of hair follicles	Skin	Pancreatic endocrine cells, Suprabasal keratinocytes, Late spermatids, Basal keratinocytes, Serous glandular cells, Basal respiratory cells	n/a	n/a	Loose anagen hair syndrome (600628), pseudofolliculitis barbae (612318)
ZNRF2	E3 ubiquitin-protein ligase ZNRF2	Q8NHG8	Intracellular	General cytoplasmic expression	Low	Microglial cells	Low	Macrophages & Microglia - Immune response (mainly)	n/a
CFAP97	Cilia- and flagella-associated protein 97	Q9P2B7	Intracellular	Ubiquitous cytoplasmic and membranous expression	Low	Early spermatids	Low	Non-specific - Transcription (mainly)	n/a
TRIM71	E3 ubiquitin-protein ligase TRIM71	Q2Q1W2	Intracellular	n/a	Testis	Extravillous trophoblasts, Spermatogonia, Horizontal cells, Alveolar cells type 2, Oocytes, Alveolar cells type 1	Low	Neurons - Mixed function (mainly)	Hydrocephalus, congenital 4; HYC4 (618667)
DENND4C	DENN domain-containing protein 4C	Q5VZ89	Membrane, Intracellular (different isoforms)	Cytoplasmic expression in most tissues	Low	Low	Low human brain regional specificity	Non-specific - Transcription (mainly)	n/a

FOXO6	Forkhead box protein O6	n/a	Intracellular	n/a	n/a	Granulosa cells, Mesothelial cells, Skeletal myocytes	Low	Choroid plexus - Cilium (mainly)	n/a
TYSND1	Peroxisomal leader peptide-processing protease	Q2T9J0	Intracellular	Cytoplasmic expression in most tissues	Low	Late spermatids, Early spermatids, Spermatocytes	Low	Non-specific - Transcription (mainly)	n/a
CLASRP	CLK4 associating serine/arginine rich protein	Q8N2M8	Intracellular	Nuclear expression in several tissues	Low	Low	Low	Non-specific – Immune response (mainly)	n/a

[a] For human motif-containing proteins with correlation scores to IC-motif $r \geq 0.7$ for the respective motif-containing peptide(s), data on protein and RNA expression were extracted from the Human Protein Atlas (proteinatlas.org). Data on protein-related human diseases derives from OMIM database (omim.org). Hypothetical proteins LOC100287739 and LOC728275 were excluded from extraction due to the absence of functional characterization.